



This is the accepted manuscript made available via CHORUS. The article has been published as:

Maximal entanglement velocity implies dual unitarity

Tianci Zhou and Aram W. Harrow

Phys. Rev. B **106**, L201104 — Published 7 November 2022

DOI: 10.1103/PhysRevB.106.L201104

Maximal Entanglement Velocity Implies Dual Unitarity

Tianci Zhou¹ and Aram W. Harrow¹

¹ Center for Theoretical Physics, Massachusetts Institute of Technology, Cambridge, Massachusetts 02139, USA (Dated: October 24, 2022)

A global quantum quench can be modeled by a quantum circuit with local unitary gates. In general, entanglement grows linearly at a rate given by entanglement velocity. Locality yields a finite light cone, which bounds the velocity. We show that the unitary interactions achieving the maximal rate must remain unitary if we exchange the space and time directions – a property known as dual unitarity. Our results are robust: approximate maximal entanglement velocity also implies approximate dual unitarity. We further show that maximal entanglement velocity is always accompanied by a specific dynamical pattern of entanglement, which yields simpler analyses of several known exactly solvable models.

Introduction. The propagation of information can never exceed the speed of light, due to Lorentz invariance. Any particle actually achieving this speed must be massless, and lower speed limits can be placed on massive particles when energy is limited. In non-relativistic systems where the speed of light is effectively infinite, the locality of the interactions poses an emergent constraint[1]. In this letter, we study the speed limit of entanglement – a measure of quantum information – in locally interacting quantum circuits. As with the speed of light, it will turn out that local unitary interactions (or "gates") that achieve the maximum velocity of spreading entanglement have a special form.

There is a natural notion of entanglement velocity in a global quantum quench[2–4]. When a short-range entangled state $|\psi_0\rangle$ is unitarily evolved, in general, a (small) subsystem Q will thermalize. After a sufficiently long time, the entanglement (or von Neumann) entropy S(Q) of the subsystem Q will saturate to its equilibrium value. To set the stage, we consider an infinite lattice qudit system in one dimension with local Hilbert space dimension q and take a semi-infinite region Q as the subsystem. We assume that the unitary evolution can thermalize the state $|\psi_0\rangle$ to infinite temperature. On the way to equilibrium, the von Neumann entropy of Q typically grows linearly in t[5–7]

$$S(Q)_t \equiv S(Q)_{\rho(t)} \equiv -\operatorname{tr}(\rho_Q \ln \rho_Q) \sim \ln(q) v_E t.$$
 (1)

The linear coefficient divided by the entropy density $\ln(q)$ has the dimension of velocity. It is thus called the entanglement velocity and denoted as v_E . A more precise definition of v_E is the asymptotic growth rate (maximized over short-range initial states)

$$v_E = \lim_{t \to \infty} \frac{S(Q)_t}{t \ln(q)}.$$
 (2)

We model spatially local interaction by a quantum circuit with local gates in a brickwork structure (Fig. 1(a)). The brickwork unitary circuit has been extensively studied in recent research about quantum chaos[8–12] and entanglement[9, 13–16], bearing fruitful results. Taking

the depth as time, the construction has a natural light cone velocity $v_{\rm LC} = 1$, so that the effective system size is at most $2v_{\rm LC}t = 2t$. This corresponds to a Hilbert space of dimension q^{2t} . The largest entanglement occurs when a q^t -dimensional subspace of Q maximally entangles with a q^t -dimensional subspace of Q's complement (Fig. 1(a)). Thus $S(Q)_t \leq t \ln q$ and $v_E \leq 1$.

In the study of quantum chaos, researchers discovered certain (generally non-integrable) brickwork circuits whose v_E is exactly 1[17]. The gate is taken to be *self dual* as we now define. We denote a two-site unitary gate as u with element $u_{ij,kl}$. By definition, we obtain an identity matrix when multiplying u with its Hermitian conjugate, *i.e.* $u_{ij,kl}u_{i'j',kl}^* = \delta_{ii'}\delta_{jj'}$. We draw this unitarity relation as

The four-leg red and blue tensors represent a two-site unitary and its complex conjugate respectively, with the top/bottom legs as row/column indices ij/kl. Contraction at the bottom represents matrix multiplication, and the two || tensors on the right denote the identities on the two sites. A dual unitary satisfies an additional dual unitarity relation

$$\begin{bmatrix}
i'_{l,i} & \rho^{j} \\
k''_{k} & l
\end{bmatrix} = k \begin{pmatrix} i' \\
k \end{pmatrix}^{i} \qquad \text{(dual unitarity)} .$$
(4)

It means that the matrix is also a unitary when viewed sideways, *i.e.* $u_{ij,kl}u_{i'j,k'l}^* = \delta_{ii'}\delta_{kk'}$. Examples of dual unitaries include the swap gate and quantum Fourier transform[18, 19], see review[12] for more constructions.

The dual unitary circuits are strongly chaotic[14, 17, 20–23]. Its auto-correlation[14, 24] and quantum butterfly effect travels at the light cone speed of 1[25](though not exclusively[26]). The spectrum form factor[20, 27] exactly reproduces the random matrix behavior. For certain solvable initial states, it has $v_E = 1[17, 28, 29]$.

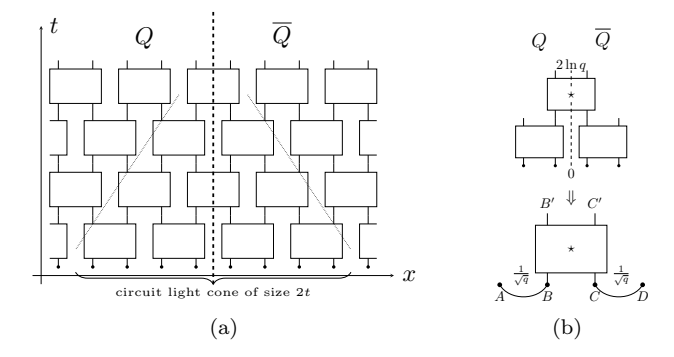


Figure 1. (a) The brickwork circuit. Solid circles at the bottom denote product initial states. The vertical dashed line cut the system into subsystem Q and \overline{Q} . The dotted line delineates the circuit light cone. (b) (top) At t=2, analysis of $S(Q)_{t=2}$ reduces to 4 qudits and 3 gates. $S(Q)_{t=2}$ is set to be the maximal $2 \ln q$. (bottom) Evolution from t=1 to t=2 with input ρ_{ABCD} and output $\rho_{AB'C'D}$.

In this letter, we ask what is required for the circuit to have $v_E = 1$. We prove two conditions: the dual unitarity (Eq. (4)) of the gate and a decoupling structure (Fig. 2(b)) of the input state. These conditions are robust: if $v_E = 1 - \eta$, they are satisfied up to error $O(\eta^{\frac{1}{2}})$ for small positive η . Furthermore, such a local decoupling structure is exact in solvable states. When acted on by an arbitrary dual unitary circuit, they yield $v_E = 1$ exactly without the need for an asymptotical limit. We will discuss later in the paper how dual unitaries are the most efficient way to produce highly entangled states.

Almost maximal growth by a gate. The entanglement velocity v_E can be thought of as the long-term average rate of entanglement growth per gate. Since the expression involves a limit, $v_E = 1$ can still be achieved if most gates have near-maximal entanglement growth.

We start here with the $v_E \leq 1$ limit. Follow the dashed line in Fig. 1(a) from the bottom to the top. Entanglement can only change when the line pierces through a unitary gate, every other time step. The maximal growth by one gate is upper bounded by $2 \ln q$ (Lemma 1 of [30]). After t time steps (assuming t even), there are t/2gates between Q and \overline{Q} , corresponding to entanglement changes $\Delta_{\tau} \equiv S(Q)_{2\tau} - S(Q)_{2\tau-1}$ for $\tau = 1, 2, \dots, t/2$. Each $\Delta_{\tau} \leq 2 \ln(q)$. On the other hand, if $v_E = 1$ then $\frac{1}{t/2}\sum_{\tau}\Delta_{\tau} \geq (1-\eta)2\ln(q)$ where $\eta \to 0$ as $t \to \infty$. Thus there exists at least one τ where the entanglement increase Δ_{τ} is $\geq (1-\eta)2\ln(q)$. As we take $t \to \infty$ this argument shows that individual gates must yield entanglement increases arbitrarily close to $2\ln(q)$. Note that the $2\ln(q)$ upper bound is not really used here. We get the existence of gates with entanglement growth $\geq (1-\eta)2\ln(q)$ just because that's the average entanglement growth. We need the upper bound only to interpret this as near-maximal.

A 4-qudit model. A simple version of the relation be-

tween dual unitarity and maximal entanglement growth can be seen in a 4-qudit example. Suppose we have $S(Q)_{t=0}=0$ and $S(Q)_{t=2}=2\ln q$ in Fig. 1(a), then for the sake of entanglement S(Q), we only need to consider 4 qudits and 3 gates(Fig. 1(b)). (Later we will generalize this to the case where the initial entanglement may be large.) We label the four qudits at the slice of t=1 as A, B, C and D. The gate evolves B and C to B' and C' (Fig. 1(b) bottom). Our assumption of maximal entanglement growth means that $S(AB') - S(AB) = 2\ln q$.

The input and output states can be determined from the entropies. We have S(AB)=0, due to the product initial state and absence of gate across AB and CD at t=1. Thus AB' is maximally mixed. By tracing out B', so is A (for t=2 and consequently for t=1). B therefore forms a Bell state with A at t=1. Similarly, C forms a Bell state with D. We denote the Bell state as a curved line connecting the qudits in Fig. 1(b) bottom (there is an ambiguity of a unitary transformation in A, but it can be removed once we obtain the RHS of Eq. (5)).

In a graphical notation similar to Eq. 3 and Eq. 4, we rewrite $\rho_{AB'}$ in two ways

$$\frac{1}{q^2} \bigcup = \frac{1}{q^2} | \mathbf{y} \otimes \mathbf{y}. \tag{5}$$

On the LHS, the input state – two separate Bell pairs – is conjugated by u (red) and u^{\dagger} (blue). Partial trace at C', D denoted by the closed loop gives $\rho_{AB'}$. The open $| \cdot |$ -shape symbol denotes the maximally mixed states at A and B'. Canceling the normalization factor $\frac{1}{q^2}$, Eq. (5) is an alternative way to write down the dual unitary condition in Eq. (4). Thus we see that maximal entanglement growth implies dual unitarity in our example.

Approximate maximal entangling. We extend the intuition in the 4-qudit toy model to the case where entanglement growth is almost maximal. This could arise if $v_E=1$ and individual gates approach but do not necessarily achieve this limit; alternately we might have v_E close to, but not equal to, 1. In Theorem 1 we will derive entropy bounds to analyze the input and output states, yielding an approximate dual unitary condition.

More formally, let us consider at time slice t there is a gate on the dashed line Fig. 1(a) which is nearly maximally entangling. The gate u acts on qudits B and C, while A (D) now denotes the collection of qudits to the left (right) of B (C)[31–35], see Fig. 2(a). Unitary gates acting exclusively on A or D do not change S(AB'), so are ignored.

Theorem 1 (proximity to dual unitarity). Let u act as in Fig. 2(a) such that

$$S(AB') - S(AB) = 2\ln q - \epsilon \tag{6}$$

then

$$\left\| \frac{1}{q} | \otimes \frac{1}{q} | - \frac{1}{q^2} \right\|_1 \le O(\epsilon^{\frac{1}{2}}) \tag{7}$$

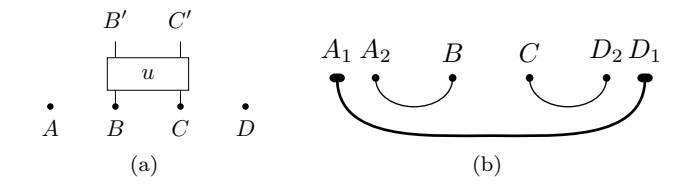


Figure 2. (a) The 4-party setup. Entanglement increases by $2 \ln q - \epsilon$ after applying unitary u on qudits B and C (Eq. (6)). A and D are auxiliary systems with arbitrary (finite) dimensions. (b) The decoupling entanglement structure. A (D) is partitioned into A_1 (D_1) and qudit A_2 (D_2). A_2B and D_2C are Bell pairs.

When $v_E = 1$, ϵ goes to zero for a sequence of gates along the dashed line in Fig. 1(a). Hence $v_E = 1$ implies that the gate is dual unitary. If $v_E = 1 - \eta$, then the entanglement growth for a sequence of gates along the dashed line can converge to $2 \ln q(1 - \eta)$. Theorem 1 indicates that the dual unitary condition is satisfied up to an error of order $\eta^{\frac{1}{2}}$.

When Eq. (7) holds, there a nearby dual unitary. We give an explicit bound for q=2 thanks to an explicit parameterization; for q>2, we know only non-explicit bounds.

Theorem 2. If u has $v_E = 1 - \eta$ for $0 < \eta < 1$, then \exists a dual unitary u_{\times} , s.t. it is close to the gate u up to an error

$$\|u - u_{\times}\|_{1} \le \begin{cases} O(\eta^{\frac{1}{4}}) & \text{if } q = 2\\ f_{q}(\eta) & \text{if } q > 2, \end{cases}$$
 (8)

where $f_q(\eta) \to 0$ as $\eta \to 0$.

The rest of this section gives a proof sketch of Theorem 1. See Supplemental Material[36] for the proof of Theorem 2.

First, we show that near-maximal entanglement increases require that B and C be nearly maximally entangled with A and D, respectively.

Lemma 1. Let u act as in Fig. 2(a) and assume entanglement growth in Eq. (6). Then

$$-S(B|A) = S(A) - S(AB) \ge \ln q - \epsilon \tag{9}$$

$$-S(D|C) = S(D) - S(CD) \ge \ln q - \epsilon. \tag{10}$$

The lemma can be proved by telescoping S(A) - S(AB') + S(AB') - S(AB) and using sub-additivity[36].

The subsystem AB contains one extra qudit (B) than A, yet its entanglement is at least $\ln q - \epsilon$ smaller. This almost maximal difference implies that $-S(B|A) \ge \ln(q) - \epsilon$ entanglement can be asymptotically distilled from the state [37, Chaps 11, 24].

Lemma 2 (local decoupling structure in input). Up to unitary transformations exclusively in A or D, the input

state ρ_{ABCD} can be approximated by

$$\sigma_{ABCD} = |\alpha_{A_2B}\rangle\langle\alpha_{A_2B}| \otimes \sigma_{A_1D_1} \otimes |\beta_{CD_2}\rangle\langle\beta_{CD_2}|$$
 (11) s.t.

$$\|\rho_{ABCD} - \sigma_{ABCD}\|_{1} \le O(\epsilon^{\frac{1}{2}}). \tag{12}$$

Here A_1, A_2 (D_1, D_2) are partitions of A (D), and A_2 (D_2) is a qudit. $|\alpha_{A_2B}\rangle$ and $|\beta_{CD_2}\rangle$ are maximally entangled, i.e. $S(A_2)_{\alpha} = S(D_2)_{\beta} = \ln q$.

Fig. 2(b) depicts the structure of σ_{ABCD} in the theorem. Using similar notation as in Eq. (5) for the Bell state, Eq. (12) can be written as

$$\|\rho_{ABCD} - \sigma_{A_1D_1} \otimes \bigcup_{A_2B}/q \otimes \bigcup_{CD_2}/q\|_1 \le O(\epsilon^{\frac{1}{2}}).$$
(13)

We use monogamy of entanglement to prove this structure, see [36] for details.

Now we discuss the constraints that apply to the output state $\rho_{AB'}$, which should be nearly maximally mixed on A_2B' after tracing out A_1 .

Lemma 3 (almost maximally mixed output). Given the configurations in Fig. 2(a) and entanglement growth in Eq. (6), we have

$$\left\| \rho_{A_1 A_2 B'} - \sigma_{A_1} \otimes \bigcup_{A_2} / q \otimes \bigcup_{B'} / q \right\|_1 \le O(\epsilon^{\frac{1}{2}}) \tag{14}$$

where | | / q | denotes a maximally mixed state, σ_{A_1} is the reduced state from σ_{ABCD} in Eq. (11).

For the proof, we can first deduce the deduce the approximate decoupling $\|\rho_{AB'} - \rho_A \otimes \mathbb{I}/q\|_1 \leq O(\epsilon^{\frac{1}{2}})$ and then replace the ρ_A by the approximate $\sigma_{A_1} \otimes \mathbb{I}_{A_2}/q$ from the known structure in Lemma 3.

With these ingredients, we can prove Theorem 1.

Proof. Taking partial trace of C'D in Eq. (13), we have the approximation from the input side,

$$\left\| \rho_{AB'} - \sigma_{A_1} \otimes \frac{1}{q^2} \right\|_{1} \leq O(\epsilon^{\frac{1}{2}}) \tag{15}$$

On the output side, we replace $\rho_{AB'}$ with the maximally mixed state in Lemma 3,

$$\left\| \sigma_{A_1} \otimes \frac{1}{q} | \otimes \frac{1}{q} | - \sigma_{A_1} \otimes \frac{1}{q^2} \right\|_{1} \le O(\epsilon^{\frac{1}{2}}) \quad (16)$$

Taking partial trace in A_1 does not increase the distance. We thus obtain Eq. (7).

Mechanism for $v_E = 1$. We have shown that dual unitarity is a necessary condition for $v_E = 1$. For sufficiency, it is known that $v_E = 1$ for translational invariant dual unitary circuits even at finite times, given special classes of "solvable" initial states [17, 23].

We enhance the results by dropping the translational invariance and prove $v_E = 1$ for solvable states through the entanglement structure developed above.

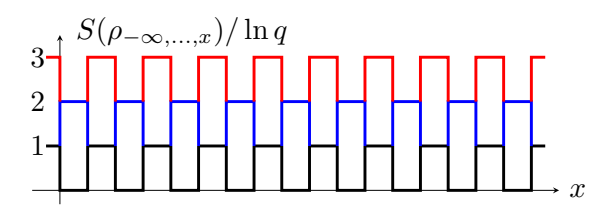


Figure 3. Entanglement entropy of sites from $-\infty$ to x in unit of $\ln q$ for t=1 (black), t=2 (blue) and t=3 (red). $v_E=1$ at finite time. At t=1, the entanglement alternates between 0 and $\ln q$. Applying dual unitary gates at the valleys relay this zigzag pattern.

Theorem 3 (dual unitarity relays the zigzag entanglement pattern). Suppose at the t=1 time slice, the entanglement across bonds alternates between $\ln q$ or 0. For any dual unitary circuits, we have at even steps:

$$S(Q)_t = t \ln q. \tag{17}$$

Proof. At t = 1, the entanglement profile is given by the black curve in Fig. 3. There are peaks whose value is $\ln q$ and valleys whose value is 0. Since the valley has $\ln q$ entanglement smaller than its neighbors (Lemma 1 with $\epsilon = 0$), the input state locally has the exact distillable entanglement structure in Fig. 2(b)(Lemma 2 with $\epsilon = 0$). When a dual unitary gate acts at the valley, dual unitarity guarantees to increase the entanglement by $2 \ln q$ (the 4-qudit model). A valley becomes a peak. In a brickwork circuit structure, the gate always acts on valleys. Thus the circuit interchanges the role of peak and valley in one step, yet still maintains the entanglement difference to be $\ln q$. For example, the red and blue lines in Fig. 3 depicts the entanglement profile at t=2and t=3. We see that the dual unitary gates can relay the zigzag entanglement pattern, while always generating $2 \ln q$ entanglement in each step, even if the gates are different across the circuit. Hence the exact relation $S(Q)_t = t \ln q$ at even steps.

We find that "solvable" states[17, 23] can initiate a zigzag pattern[36] (blue line in Fig. 3.) Thus its entanglement growth can achieve $v_E=1$ without the need for an asymptotic limit. We conjecture that the zigzag pattern can be dynamically generated in a dual unitary circuit even if absent in the initial state, thus achieving $v_E=1$ as $t\to\infty$.

Discussion.— In quantum simulation experiments, it is desirable to create entangled states as quickly as possible to complete the operations within the coherence time and to reduce errors. Theorem 1 suggests *only* (approximate) dual unitarity gives the (nearly) maximal entanglement growth rate. In fact, in the random circuit sampling experiment by the Google Quantum AI group[38], the original choice of CZ gate was replaced by a dual unitary gate in order to better resist classical simulation; see Section VIII.A of [36] for details.

A random pure state on two qudits has entanglement $\ln q - \mathcal{O}(1)$. It is an approximate unitary from one qudit to the other: the expected fidelity with a maximally entangled state is $\frac{8}{3\pi} + \mathcal{O}(q^{-2})[36]$. Similarly a random unitary (brickwork) circuit has $v_E \sim 1 - \mathcal{O}(\frac{1}{\ln(q)})$ at large q[39, 40]. Each gate increases entanglement by $2 \ln q - \epsilon$, with ϵ an $\mathcal{O}(1)$ number in q. By Theorem 1, we infer that a random unitary has an $\mathcal{O}(1)$ distance to a dual unitary. This is consistent with expected fidelity $\frac{8}{3\pi} + \mathcal{O}(q^{-2})[36]$. Thus in both cases, we see an $\mathcal{O}(1)$ deviation from maximal entanglement, whether measured in entropy or fidelity.

In numerical simulations of quantum chaos, pseudorandom choices of the gate parameters can accidentally lead to $v_E \approx 1[41-43]$. Our theorem indicates that it is approximately a dual unitary (Sec. VIII.B of [36]), which would hinder typical behaviors of chaotic dynamics from being observed at numerically accessible system sizes.

Lemma 2 characterizes the local decoupling structure of the state to have maximal entanglement growth. Instead of relying on translational invariance, in Theorem 3 we use the decoupling structure to demonstrate why $v_E=1$ even at finite times for arbitrary dual unitary circuits acting on solvable states. We believe that such a zigzag structure can be dynamically generated even when the initial states are not "solvable", see proof for a subset of dual unitaries in Ref. [44].

Next we consider continuous setups. When space is discrete and time is continuous, the question of maximal entanglement velocity is known as the "small incremental entangling" (SIE) problem [31, 33, 35, 45]. Using the 4-party setup in Fig. 2 with $u=e^{-iHt}$, the best known SIE bound is $\frac{dS(AB)_t}{dt} \leq 8\|H\|\ln(q)$, which resembles the corresponding discrete-time bound, up to O(1) factors [45]. However, the structure of the optimal entangling state in continuous time is unknown. The locally decoupling state in Fig. 2(b) maximizes entanglement growth in discrete time but has $\frac{dS(AB)_t}{dt}=0$ in continuous time for any H. Further developing connections between these settings is an intriguing direction for study.

In a quantum field theory, both space and time are continuous. In Lorentz-invariant theories, we also have $v_E \leq v_{\rm LC}$ and the proofs[2, 4] are quite similar to our entropy bound estimates in [36]. There are examples, such as conformal field theories in 1+1 dimension that have $v_E = v_{\rm LC}$. It is natural to attempt to extend our results to this setting; however, defining the right field-theoretic analogue of dual unitarity is an open question.

In d dimensional space-time, holographic systems which are believed to be strongly chaotic have [46, 47]

$$v_E = \frac{\sqrt{d(d-2)^{\frac{1}{2} - \frac{1}{d}}}}{(2(d-1))^{1 - \frac{1}{d}}}$$
 and $v_{LC} = \sqrt{\frac{d}{2(d-1)}}$. (18)

When d = 1 + 1, $v_E = v_{LC} = 1$ as in the discrete case, but when d > 1 + 1, $v_E < v_{LC}$. We note that our theorem

only gives the necessary condition for $v_E = v_{\rm LC}$ without showing that circuits achieving $v_E = v_{\rm LC}$ in fact exist for d > 1+1. There are two important questions in higher dimensions (i.e. d > 1+1) for both the continuum and discrete cases: (1) is the maximal v_E strictly less than $v_{\rm LC}$?; and (2) if so, which gates/Hamiltonians can achieve maximal v_E ? We conjecture that the dual unitary gates still give the maximal possible rate, but the rate itself could depend on the lattice structure in the discrete case and the geometry of the cut in both the discrete and continuum cases.

Finally, we may exploit the small temporal (operator) entanglement of the (almost maximally) mixed output state (AB' or C'D) in a matrix product state-based algorithm. We leave this to future work.

Acknowledgments: Both authors were funded by NTT Research Award AGMT DTD 9.24.20. AWH is also supported by NSF grants CCF-1729369 (STAQ), PHY-1818914 (EPiQC) and OMA-2016245 (QLCI CIQC). We thank Yichen Huang for helping check the proof of Theorem 1, and Daniel Ranard for suggesting the continuity argument for q>2 in Theorem 2. We thank Pavel Kos, Austen Lamacraft, Pieter Claeys, Wen Wei Ho, Bruno Bertini, Balázs Pozsgay and Jon Tyson for commenting on the manuscript. We thank Wen Wei Ho and Bruno Bertini for explaining the properties of the solvable MPS ansatz to us. We thank Xun Gao, Sergio Boxio for a discussion of the gates used in the Google Quantum AI experiment.

- E. H. Lieb and D. W. Robinson, The finite group velocity of quantum spin systems, Commun.Math. Phys. 28, 251 (1972).
- [2] H. Casini, H. Liu, and M. Mezei, Spread of entanglement and causality, J. High Energ. Phys. 2016 (2016), 10.1007/jhep07(2016)077.
- [3] H. Liu and S. J. Suh, Entanglement Tsunami: Universal Scaling in Holographic Thermalization, Phys. Rev. Lett. 112, 011601 (2014).
- [4] T. Hartman and N. Afkhami-Jeddi, Speed Limits for Entanglement, arXiv:1512.02695 [hep-th] (2015).
- [5] P. Calabrese and J. Cardy, Quantum quenches in extended systems, J. Stat. Mech. 2007, P06008 (2007).
- [6] P. Calabrese and J. Cardy, Quantum quenches in 1 + 1 dimensional conformal field theories, J. Stat. Mech. 2016, 064003 (2016).
- [7] H. Kim and D. A. Huse, Ballistic spreading of entanglement in a diffusive nonintegrable system, Phys. Rev. Lett. 111, 127205 (2013).
- [8] A. Nahum, S. Vijay, and J. Haah, Operator spreading in random unitary circuits, Phys. Rev. X 8, 021014 (2018).
- [9] C. W. von Keyserlingk, T. Rakovszky, F. Pollmann, and S. L. Sondhi, Operator hydrodynamics, OTOCs, and entanglement growth in systems without conservation laws, Phys. Rev. X 8, 021013 (2018).
- [10] T. Rakovszky, F. Pollmann, and C. W. von Keyserlingk,

- Diffusive hydrodynamics of out-of-time-ordered correlators with charge conservation, Phys. Rev. X 8, 031058 (2018).
- [11] V. Khemani, A. Vishwanath, and D. A. Huse, Operator spreading and the emergence of dissipative hydrodynamics under unitary evolution with conservation laws, Phys. Rev. X 8, 031057 (2018).
- [12] M. Borsi and B. Pozsgay, Remarks on the construction and the ergodicity properties of dual unitary quantum circuits (with an Appendix by Roland Bacher and Denis Serre), arXiv:2201.07768 [cond-mat, physics:nlin, physics:quant-ph] (2022).
- [13] A. Nahum, J. Ruhman, S. Vijay, and J. Haah, Quantum entanglement growth under random unitary dynamics, Phys. Rev. X 7, 031016 (2017).
- [14] B. Bertini, P. Kos, and T. Prosen, Exact Correlation Functions for Dual-Unitary Lattice Models in \$1+1\$ Dimensions, Phys. Rev. Lett. 123, 210601 (2019).
- [15] A. M. Dalzell, A. W. Harrow, D. E. Koh, and R. L. La Placa, How many qubits are needed for quantum computational supremacy? Quantum 4, 264 (2020).
- [16] A. Chan, A. De Luca, and J. T. Chalker, Solution of a Minimal Model for Many-Body Quantum Chaos, Phys. Rev. X 8, 041019 (2018).
- [17] B. Bertini, P. Kos, and T. Prosen, Entanglement Spreading in a Minimal Model of Maximal Many-Body Quantum Chaos, Phys. Rev. X 9, 021033 (2019).
- [18] J. Tyson, Operator-Schmidt decomposition of the quantum Fourier transform on n1 n2, J. Phys. A: Math. Gen. 36, 6813 (2003).
- [19] J. E. Tyson, Operator-Schmidt decompositions and the Fourier transform, with applications to the operator-Schmidt numbers of unitaries, J. Phys. A: Math. Gen. 36, 10101 (2003).
- [20] B. Bertini, P. Kos, and T. Prosen, Exact Spectral Form Factor in a Minimal Model of Many-Body Quantum Chaos, Phys. Rev. Lett. 121, 264101 (2018).
- [21] T. Prosen, Many-body quantum chaos and dual-unitarity round-a-face, Chaos 31, 093101 (2021).
- [22] S. Gopalakrishnan and A. Lamacraft, Unitary circuits of finite depth and infinite width from quantum channels, Phys. Rev. B 100, 064309 (2019).
- [23] L. Piroli, B. Bertini, J. I. Cirac, and T. Prosen, Exact dynamics in dual-unitary quantum circuits, Phys. Rev. B 101, 094304 (2020).
- [24] P. Kos, B. Bertini, and T. Prosen, Correlations in Perturbed Dual-Unitary Circuits: Efficient Path-Integral Formula, Phys. Rev. X 11, 011022 (2021).
- [25] B. Bertini and L. Piroli, Scrambling in random unitary circuits: Exact results, Phys. Rev. B 102, 064305 (2020).
- [26] P. W. Claeys and A. Lamacraft, Maximum velocity quantum circuits, Phys. Rev. Research 2, 033032 (2020).
- [27] B. Bertini, P. Kos, and T. Prosen, Random Matrix Spectral Form Factor of Dual-Unitary Quantum Circuits, Commun. Math. Phys. 387, 597 (2021).
- [28] J. Bensa and M. Žnidarič, Fastest Local Entanglement Scrambler, Multistage Thermalization, and a Non-Hermitian Phantom, Phys. Rev. X 11, 031019 (2021).
- [29] B. Bertini, P. Kos, and T. Prosen, Operator Entanglement in Local Quantum Circuits I: Chaotic Dual-Unitary Circuits, SciPost Physics 8, 067 (2020).
- [30] C. Bennett, A. Harrow, D. Leung, and J. Smolin, On the capacities of bipartite hamiltonians and unitary gates, IEEE Trans. Inform. Theory 49, 1895 (2003).

- [31] S. Bravyi, Upper bounds on entangling rates of bipartite hamiltonians, Phys. Rev. A 76, 052319 (2007).
- [32] E. H. Lieb and A. Vershynina, Upper bounds on mixing rates, QIC 13, 986 (2013).
- [33] K. Van Acoleyen, M. Marin, and F. Verstraete, Entanglement rates and area laws, Phys. Rev. Lett. 111, 170501 (2013).
- [34] M. Mariën, K. M. R. Audenaert, K. Van Acoleyen, and F. Verstraete, Entanglement Rates and the Stability of the Area Law for the Entanglement Entropy, Commun. Math. Phys. 346, 35 (2016).
- [35] S. G. Avery and M. F. Paulos, Universal bounds on the time evolution of entanglement entropy, Phys. Rev. Lett. 113, 231604 (2014).
- [36] See the Supplemental Material for more details about the proofs.
- [37] M. M. Wilde, Quantum Information Theory (Cambridge University Press, Cambridge, 2013).
- [38] F. Arute, K. Arya, R. Babbush, D. Bacon, J. C. Bardin, R. Barends, R. Biswas, S. Boixo, F. G. S. L. Brandao, D. A. Buell, B. Burkett, Y. Chen, Z. Chen, B. Chiaro, R. Collins, W. Courtney, A. Dunsworth, E. Farhi, B. Foxen, A. Fowler, C. Gidney, M. Giustina, R. Graff, K. Guerin, S. Habegger, M. P. Harrigan, M. J. Hartmann, A. Ho, M. Hoffmann, T. Huang, T. S. Humble, S. V. Isakov, E. Jeffrey, Z. Jiang, D. Kafri, K. Kechedzhi, J. Kelly, P. V. Klimov, S. Knysh, A. Korotkov, F. Kostritsa, D. Landhuis, M. Lindmark, E. Lucero, D. Lyakh, S. Mandrà, J. R. McClean, M. McEwen, A. Megrant, X. Mi, K. Michielsen, M. Mohseni, J. Mutus, O. Naaman, M. Neeley, C. Neill, M. Y. Niu, E. Ostby, A. Petukhov, J. C. Platt, C. Quin-

- tana, E. G. Rieffel, P. Roushan, N. C. Rubin, D. Sank, K. J. Satzinger, V. Smelyanskiy, K. J. Sung, M. D. Trevithick, A. Vainsencher, B. Villalonga, T. White, Z. J. Yao, P. Yeh, A. Zalcman, H. Neven, and J. M. Martinis, Quantum supremacy using a programmable superconducting processor, Nature 574, 505 (2019).
- [39] C. Jonay, D. A. Huse, and A. Nahum, Coarse-grained dynamics of operator and state entanglement, arXiv:1803.00089 [cond-mat, physics:hep-th, physics:nlin, physics:quant-ph] (2018).
- [40] T. Zhou and A. Nahum, Emergent statistical mechanics of entanglement in random unitary circuits, Phys. Rev. B 99, 174205 (2019).
- [41] H. Kim, T. N. Ikeda, and D. A. Huse, Testing whether all eigenstates obey the eigenstate thermalization hypothesis, Physical Review E 90, 052105 (2014).
- [42] L. Zhang, H. Kim, and D. A. Huse, Thermalization of entanglement, Physical Review E 91, 062128 (2015).
- [43] T. Zhou and D. J. Luitz, Operator entanglement entropy of the time evolution operator in chaotic systems, Phys. Rev. B 95, 094206 (2017).
- [44] A. Foligno and B. Bertini, Growth of entanglement of generic states under dual-unitary dynamics, (2022), arXiv:2208.00030 [cond-mat, physics:hep-th, physics:math-ph, physics:quant-ph].
- [45] K. M. R. Audenaert, Quantum Skew Divergence, Journal of Mathematical Physics 55, 112202 (2014).
- [46] M. Mezei, On entanglement spreading from holography, arXiv:1612.00082 [cond-mat, physics:hep-th] (2016).
- [47] M. Mezei and D. Stanford, On entanglement spreading in chaotic systems, arXiv preprint arXiv:1608.05101 (2016).